ON THE VALIDITY OF THE DOUBLE INTEGRATOR APPROXIMATION IN DEEP SPACE FORMATION FLYING

Daniel P. SCHARF, Fred Y. HADAEGH, and Bryan H. KANG

Jet Propulsion Laboratory
California Institute of Technology
4800 Oak Grover Dr.
Pasadena, CA 91109

ABSTRACT *- Free-flying models are commonly used for path planning and open loop control design (i.e., guidance design) and translational feedback control design (i.e., control design) for deep space precision formation flying. The free flying model, essentially a double integrator, results from discarding small terms in the relative spacecraft equations of motion. While the magnitude of these discarded terms may be small, one must show that their dynamic effects are small as compared to the precision performance requirements. We do so by deriving a theoretical method for bounding the difference between the solution of a nonlinear truth model of the relative translational spacecraft dynamics and a simplified linear time-invariant model. Presently, the method incorporates feedforward and static output feedback control. The method is applied to a Terrestrial Planet Finder-based example. Using only feedforward control (guidance) the free-flying model and a Hill-Clohessy-Wiltshire Equations-based model are shown to be accurate to* $1\,cm$ *for up to 4 and 30 hours, respectively. Also shown is that the simplest free-flying model may not be sufficient for low-gain feedback control design—closed-loop tracking errors can be as large as 8 meters.*

1 - INTRODUCTION

Terrestrial Planet Finder (TPF) requires relative spacecraft positions to be controlled to the level of millimeters [Beic 99], that is, it requires *precision* formation flying. A common practice in designing trajectories and control algorithms for precision formations is to first linearize the "truth" model.[1] For example, when a reference or "leader" spacecraft is in a circular orbit the Hill-Clohessy-Wiltshire (HCW) Equations can be used to design optimal controllers or trajectories for a formation [DeCo 91; Hada 00]. A further simplification results when the particular circular solar orbit baselined for TPF is considered. A routine analysis shows that the magnitude of the solar pressure, third body perturbations and differential solar gravity terms are orders of magnitude less than thruster accelerations [Hada 00]. Discarding these small terms results in the commonly called *free-flying model*, in which the relative spacecraft dynamics reduce to the standard double integrator form [Rao 01; Bear 01; Mesb 01; Hada 01; Wang 99].

It is not sufficient, however, to only consider the magnitude of discarded terms. One must show that their dynamic *effects* are small compared to the performance requirements. This process is normally addressed through numerical validation: trajectories are refined using shooting methods and controllers are exhaustively simulated on the truth model.

In contrast to numerical validation, this paper's contribution is a theoretical method for validating trajectories and controllers designed using simplified models. We derive upper bounds for the difference between the state of a linear time-invariant (LTI) model, such as the HCW Equations, and a nonlinear truth model. This difference is the "error" incurred by using a simplified model. Control inputs are of the form $u_{ff}(t) + Ky$ where $u_{ff}(t)$ is a continuous feedforward control, y is a measurement and K is a constant gain matrix. See Figure 1 for a graphical statement of the problem. Trajectory design is included by setting $K = 0$.

[1] See Ref. [deQu 00] for examples of nonlinear control design using a nonlinear model.

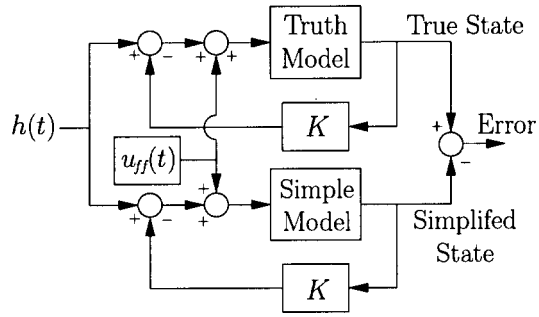

Given $u_{ff}(t)$, K and reference $h(t)$ designed using the simplified model, bound the error.

Fig. 1: Block Diagram for Error Bounding Problem Statement

The error between the truth and simplified models is shown to be governed by an LTI differential equation with a "disturbance" that depends on the state of the truth model (true state). Error bounds are obtained via a "bootstrapping" process in which a bound on the true state is first *assumed*. This assumed bound is used to bound the "disturbance" in the error dynamics. Next, this disturbance bound is used in turn to bound the error. Finally, the assumed true state is verified by ensuring that the assumed bound is greater than the just calculated error bound plus a bound on the simplified model's state.

The next section presents the truth model and derives via Taylor expansions various simplified models for deep space formation flight. This derivation includes an order of magnitude analysis. Then general bounds for the difference (error) between a nonlinear model and an LTI model are derived. Finally, the error bounds are calculated and compared to numerically simulated errors for a preliminary TPF design.

Addressing notation, geometric vectors and tensors are denoted by bold lower and upper case letters, respectively, e.g. $\boldsymbol{\rho}$ and $\mathbf{Q}$. Representations of these objects in specific coordinate frames—vectors and matrices—are given by the corresponding unbolded symbol, e.g. ρ and Q. $|\cdot|$ is the Euclidean length of a geometric vector. $\|\cdot\|$ is the vector 2-norm when applied to vectors, and the spectral norm when applied to matrices.

2 - FORMATION TRANSLATIONAL DYNAMICS

To derive the relative dynamics, a formation frame is introduced. Consider Fig. 2 in which "S/C" stands for spacecraft. An inertial frame $\mathcal{F}_I$ with origin O_I is located at the center of the Sun. The formation frame $\mathcal{F}_F$, based on an Earth-trailing orbit, has its origin moving in a circular orbit at 1 AU, i.e., $\mathbf{r}_F$ is the circular solution to the 2-Body Problem with the Sun as the central body. $\mathcal{F}_F$ is translating but not rotating with respect to $\mathcal{F}_I$.

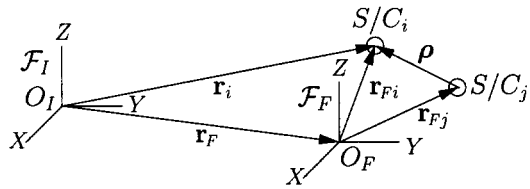

Fig. 2: Frames for Formation Dynamics

The translational equation of motion for the ith spacecraft, $i = 1, 2, ...,$ is taken from [Hada 00]:

$$\ddot{\mathbf{r}}_i = -\mu_s \frac{\mathbf{r}_i}{|\mathbf{r}_i|^3} + \mathbf{b}_i + \mathbf{g}_i + \mathbf{u}_i \tag{1}$$

where $\mathbf{r}_i$ is the position vector of the spacecraft with respect to O_I, $\mathbf{b}_i$ is the acceleration due to solar pressure, $\mathbf{g}_i$ is the acceleration due to the gravitational attraction of the planets (3^{rd} body effects) and $\mathbf{u}_i$ is the control input divided by the mass.

Considering only specular reflection and assuming the spacecraft have sun shades that always point directly at the Sun, the solar pressure term is given by [Vall 97]

$$\mathbf{b}_i = \frac{2S_f A(1\text{AU})^2}{mc} \frac{\mathbf{r}_i}{|\mathbf{r}_i|^3} = \beta_i \frac{\mathbf{r}_i}{|\mathbf{r}_i|^3}$$

where β_i is referred to as the solar pressure coefficient, the factor of 2 is from assuming perfect reflectivity, S_f is the average solar flux at 1 AU (1353 W/m^2), A is the area of the sun shade, c is the speed of light, m is the spacecraft mass, assumed constant, and the squared term accounts for the decrease in energy flux with distance from the Sun.

To derive the relative spacecraft dynamics truth model, we start with the dynamics of the position of spacecraft i with respect to O_F, denoted $\mathbf{r}_{Fi} = \mathbf{r}_i - \mathbf{r}_F$. For many deep space formations $|\mathbf{r}_{Fi}|$ is less than a few hundred kilometers over the time scales of interest, whereas $|\mathbf{r}_F| \approx 1$ AU. Therefore, we Taylor expand $1/|\mathbf{r}_i|^3$. Define the tensor $\mathbf{Q}_\mathbf{r} \triangleq (\mathbf{1} - 3\hat{\mathbf{r}}\hat{\mathbf{r}})$ where $\mathbf{1}$ is the unit tensor, $\hat{\mathbf{r}}$ is the unit vector of $\mathbf{r}$ and $\mathbf{rr}$ is a direct product. The Taylor expansion results in

$$\ddot{\mathbf{r}}_{Fi} = -\frac{\mu_s}{|\mathbf{r}_F|^3}\mathbf{Q}_{\mathbf{r}_F}\mathbf{r}_{Fi} + \frac{\beta_i}{|\mathbf{r}_F|^3}\left(\mathbf{r}_F + \mathbf{Q}_{\mathbf{r}_F}\mathbf{r}_{Fi}\right) - \sum_{k\in\text{planets}} \frac{\mu_k}{|\mathbf{r}_{kF}|^3}\left(\mathbf{r}_{kF} + \mathbf{Q}_{\mathbf{r}_{kF}}\mathbf{r}_{Fi}\right) + \mathbf{u}_i + \mathcal{E}_i \qquad (2)$$

where $\mathcal{E}_i$ is the combined remainder from all the Taylor expansions and μ_k and $\mathbf{r}_{kF}$ are, respectively, the gravitational parameter of- and the position of O_F with respect to the planets in the sum. When represented in a certain rotating frame, the first term on the right hand side yields the HCW Equations. Since the Taylor remainders are retained, (2) is still the full, nonlinear model; only its form has been changed.[2]

As in Fig. 2, $\boldsymbol{\rho} = \mathbf{r}_{Fi} - \mathbf{r}_{Fj}$, and so the relative dynamics are obtained by subtracting (2) with i replaced by j from itself:

$$\ddot{\boldsymbol{\rho}} = -\frac{\mu_s}{|\mathbf{r}_F|^3}\mathbf{Q}_{\mathbf{r}_F}\boldsymbol{\rho} + \left(\Delta\beta\frac{\mathbf{r}_F}{|\mathbf{r}_F|^3} + \frac{\beta_i}{|\mathbf{r}_F|^3}\mathbf{Q}_{\mathbf{r}_F}\boldsymbol{\rho} + \frac{\Delta\beta}{|\mathbf{r}_F|^3}\mathbf{Q}_{\mathbf{r}_F}\mathbf{r}_{Fj}\right) - \sum_{k\in\text{planets}} \frac{\mu_k}{|\mathbf{r}_{kF}|^3}\mathbf{Q}_{\mathbf{r}_{kF}}\boldsymbol{\rho} + (\mathbf{u}_i - \mathbf{u}_j) + (\mathcal{E}_i - \mathcal{E}_j) \qquad (3)$$

where $\Delta\beta = \beta_i - \beta_j$. (3) is the truth model and it is in a form that allows the effects of the nonlinearities to be quantified. The three solar pressure terms (terms including "β") are referred to as, in order: *I)* the DC term, *II)* the Q term, and *III)* the Offset term. The Offset term and the remainder terms, $\mathcal{E}_i$ and $\mathcal{E}_j$, depend on $\mathbf{r}_{Fj}$. (3)'s derivation is similar to a derivation in Ref. [Vass 85], except that all terms have been retained—quantifying their effects is our aim.

By assumption $|\mathbf{r}_F| = 1$ AU. Further assume $|\boldsymbol{\rho}| \leq 1\,km$, which is the case for TPF, and $|\mathbf{r}_{Fj}| \leq 1\,km$ (the level of inertial positioning accuracy for TPF may vary as TPF designs mature). Note $\|\mathbf{Q}_\mathbf{r}\| = 2$ for all $\mathbf{r}$. Table 1 shows upper bounds on the terms of the truth model (3) for TPF and StarLight (a possible TPF precursor) designs. Briefly, spacecraft masses range from 400 to 700 kg, sun shade diameters from 3 to 15 m and thrusters from 7.5 to 100 mN. Table 1 shows that the DC term dominates all non-thruster terms by at least four orders of magnitude. Also, the solar gravity term, the largest term on the right-hand side of (3) that is a function of $\boldsymbol{\rho}$, is six orders of magnitude less than the thruster accelerations.

These comparisons motivate three free-flying models: a model with no disturbance (n-model), a model with a constant (or 0th order) approximation to the DC term (p_0-model), and a model with the full DC term (p_∞-model). The n-model is a pure double integrator. For the p_0-model, without loss of generality, a representation in $\mathcal{F}_I$ of $\mathbf{r}_F$ is $\mathrm{r}_F = (1\text{AU})[\,\cos(\omega_E t)\;\sin(\omega_E t)\;0\,]^T$. A 0^{th} order approximation to the DC term, d_{sp}, is $d_{sp}^{(0)} = \Delta\beta/|\mathbf{r}_F|^2\,[\,1\;0\;0\,]^T$. Letting $\mathbf{r}^{(k)}$ be the kth order time-varying geometric vector comprising $\mathbf{r}$, the free flying models are

$$\ddot{\boldsymbol{\rho}}_n = (\mathbf{u}_i - \mathbf{u}_j)\,, \quad \ddot{\boldsymbol{\rho}}_{p_0} = (\mathbf{u}_i - \mathbf{u}_j) + \boldsymbol{d}_{sp}^{(0)}\,, \quad \text{and} \quad \ddot{\boldsymbol{\rho}}_{p_\infty} = (\mathbf{u}_i - \mathbf{u}_j) + \boldsymbol{d}_{sp}\,.$$

We also consider a non-free-flying model that includes the full solar gravity term. The HCW Equations-based[3] g_∞-model is

$$\ddot{\boldsymbol{\rho}}_{g_\infty} = (\mathbf{u}_i - \mathbf{u}_j) - \frac{\mu_s}{|\mathbf{r}_F|^3}\mathbf{Q}_{\mathbf{r}_F}\boldsymbol{\rho}_{g_\infty} + \boldsymbol{d}_{sp}\,.$$

[2]Taylor expansions, however, are not universally valid. The condition $|\mathbf{r}_{Fi}|/|\mathbf{r}_{lF}| < 1$ is sufficient for the validity of (2), where l can stand for any of the planets or the Sun.

[3]Though this model is essentially the HCW Equations, it describes the relative dynamics between two spacecraft neither of which is in a circular orbit.

Table 1: Bounds in m/s^2 on Terms[a] in Expanded Relative Dynamics for Starlight and TPF for $|\mathbf{r}_F| = 1$ AU and $|\mathbf{r}_{Fj}|$, $|\boldsymbol{\rho}| \leq 1\,km$.

Term	Starlight	TPF
One Thruster	2.0e-5	1.5e-4
Solar Pressure DC term	2.4e-7	7.3e-7
Solar Gravity	8.0e-11	same
Terran $10°$ Separation	4.5e-14	same
Gravity $35°$ Separation	1.1e-15	same
Max. Venusian Gravity	9.2e-15	same
Solar Pressure Q term	2.3e-15	3.0e-14
Solar Pressure Offset term	2.7e-15	9.7e-15
Max. Jovian Gravity	1.0e-15	same
Max. Martian Gravity	1.8e-16	same
Max. Mercurial Gravity	5.8e-17	same
$\mathcal{E}_i - \mathcal{E}_j$	1.1e-17	1.1e-17

[a] Planetary terms with maximum accelerations of less than 1e-18 m/s^2 are omitted.

All of these simplified models for the relative spacecraft state can be propagated without knowing the inertial state of either spacecraft. In the truth model (3), however, $\mathbf{r}_{Fj}$ appears in addition to $\boldsymbol{\rho}$. The truth model actually consists of (3) *and* (2), the latter with i replaced by j. More generally, the state vector of a formation consists of a spanning set of relative spacecraft states and the inertial state of one spacecraft. The former portion of the formation state is referred to as the *relative state*, and the latter as the *inertial state*. The inertial state is *not* the formation state represented in an inertial coordinate frame.

We now introduce some notation. Bounding the error in the simplified relative state models requires four states. Two are the true relative and inertial states, x and x_I, respectively. In our case, $x = [\rho^T \ \dot{\rho}^T]^T$ and $x_I = [\mathrm{r}_{Fj}^T \ \dot{\mathrm{r}}_{Fj}^T]^T$. The other two states are the simplified relative and inertial states, x_s and $x_{I,s}$, respectively. In our case, $x_s = [\rho_n^T \ \dot{\rho}_n^T]^T$, for example, and $x_{I,s} = [\mathrm{r}_{Fj,s}^T \ \dot{\mathrm{r}}_{Fj,s}^T]^T$, where $\mathrm{r}_{Fj,s}$ is the position of spacecraft j with respect to O_F given by the simplified model

$$\ddot{\mathbf{r}}_{Fj,s} = \frac{-(\mu_s - \beta_j)}{|\mathbf{r}_F|^3}\mathbf{Q}_{\mathbf{r}_F}\mathbf{r}_{Fj,s} + \frac{\beta_j}{|\mathbf{r}_F|^3}\mathbf{r}_F - \sum_{k\in\text{planets}} \frac{\mu_k}{|\mathbf{r}_{kF}|^3}\mathbf{r}_{kF} + u_j\,. \tag{4}$$

3 - ERROR ANALYSIS

The previous models may be described with the following generalized equations:

$$\begin{aligned} \dot{x} &= Ax + Bu_r + \mathcal{D}(t,x,x_I) & \dot{x}_I &= A_I x_I + B_I u_I + \mathcal{D}_I(t,x_I) \\ y &= Cx & y_I &= C_I x_I \\ \dot{x}_s &= A_s x_s + Bu_{r,s} + \mathcal{D}_s(t) & \dot{x}_{I,s} &= A_{I,s}x_{I,s} + B_I u_{I,s} + \mathcal{D}_{I,s}(t) \\ y_s &= Cx_s & y_{I,s} &= C_I x_{I,s} \end{aligned}$$

where the y's are the outputs available for feedback (assumed not to explicitly depend on u's, i.e., $D = 0$) the $\mathcal{D}$'s are time varying "disturbances"—disturbances, true inertial state terms, all nonlinear terms and those linear terms that can not be rendered time-invariant are all lumped into them. u_I is the control of the jth spacecraft, whereas u_r is the differential control between the ith and jth spacecraft. In putting (3) in the form above, the geometric vectors are represented in the HCW coordinate frame as then $\mathrm{Q}_{\mathrm{r}_F}$ is constant. However, the linear planetary terms, those involving $\mathrm{Q}_{\mathrm{r}_{kF}}$, are time varying and so become part of $\mathcal{D}(t,x,x_I)$.

Let the error incurred in the relative and inertial states due to using simplified models be $\Lambda = x - x_s$ and $\Lambda_I = x_I - x_{I,s}$, respectively. The equation for Λ_I has the same form as the

equation for Λ and so we only consider Λ. Subtracting the equation for $\dot{x}_s$ from the equation for $\dot{x}$ and substituting for u and u_s yields

$$\begin{aligned}\dot{\Lambda} &= (A_s + BKC)\Lambda + \{\mathcal{D}(t, x, x_I) - \mathcal{D}_s(t) + (A - A_s)x\} \\ &= \widetilde{A}\Lambda + \Gamma\,. \end{aligned} \tag{5}$$

Bounding the error in the simplified relative state, Λ, is complicated by the fact that (5) depends on the true inertial state, x_I. Hence, the true inertial state must also be bounded. Let $\bar{\cdot}$ denote a constant upper bound of $\|\cdot\|$ and $\bar{\cdot}(t)$ denote a time varying upper bound of $\|\cdot\|$, both bounds valid over a time interval that must be specified. With this notation, the error bounding process is described in detail in Table 2. The equation used to generate $\bar{x}_s(t)$ in Step 6) of the table is presented next, followed by two methods for bounding Λ (Step 8). The same equation and methods are used to calculate $\bar{x}_{I,s}(t)$ in Step 2) and bound Λ_I in Step 4), the only difference is that subscripted I's must be added to all quantities.

The following notation is useful in deriving tighter bounds. Let $[\,\cdot\,]_m$, $m = 1, 2$, be the mth 3-vector of the vector argument. Since they appear so often, we use λ and $\dot{\lambda}$ for $[\Lambda]_1$ and $[\Lambda]_2$. For matrices, $[\,\cdot\,]_{m,n}$, $m, n = 1, 2$, is the m-by-nth 3-by-3 submatrix of the argument.

3.1 - Bounding the Simplified Relative States

Let the initial conditions over which the controller (trajectory) is to be validated be specified as a nominal initial condition $x^*(0)$ plus a variation $\Delta x(0)$. Similarly, let the disturbance be given by a nominal disturbance $\mathcal{D}_s^*(t)$ plus a variation $\Delta\mathcal{D}_s$. Then from the Variation of Constants equation with $u = u_{ff} + Ky_s$, we have

$$\bar{x}_s(t) = \left\| e^{\widetilde{A}t}x^*(0) + \int_0^t e^{\widetilde{A}(t-\sigma)}(Bu_{ff}(\sigma) + \mathcal{D}_s^*(\sigma))\,\mathrm{d}\sigma \right\| + \|e^{\widetilde{A}t}\|\,\overline{\Delta x(0)} + \int_0^t \|e^{\widetilde{A}\sigma}\|\,\mathrm{d}\sigma\,\overline{\Delta\mathcal{D}}_s, \tag{6}$$

A tighter bound can often be obtained by calculating last two terms on the right-hand side of (6) as, respectively,

$$(\|[e^{\widetilde{A}t}]_{1,1}\| + \|[e^{\widetilde{A}t}]_{2,1}\|)\overline{[\Delta x(0)]}_1 + (\|[e^{\widetilde{A}t}]_{1,2}\| + \|[e^{\widetilde{A}t}]_{2,2}\|)\overline{[\Delta x(0)]}_2\,, \text{ and}$$

$$\overline{[\Delta\mathcal{D}_s]}_1 \int_0^t (\|[e^{\widetilde{A}\sigma}]_{1,1}\| + \|[e^{\widetilde{A}\sigma}]_{2,1}\|)\,\mathrm{d}\sigma + \overline{[\Delta\mathcal{D}_s]}_2 \int_0^t (\|[e^{\widetilde{A}\sigma}]_{1,2}\| + \|[e^{\widetilde{A}\sigma}]_{2,2}\|)\,\mathrm{d}\sigma.$$

3.2 - Method 1

Method 1 is primarily used for validating controllers. Given verified values of $\bar{x}$ and $\bar{x}_I$ (see Table 2), a value for $\overline{\Gamma}$ can be calculated. Since $x(0) = x_s(0)$, $\Lambda(0) = 0$. From (5) and the Variation of Constants equation we have

$$\|\Lambda(t)\| \le \overline{\Gamma}\int_0^t \|e^{\widetilde{A}\sigma}\|\,\mathrm{d}\sigma, \tag{7.a}$$

$$\|\lambda(t)\| \le \overline{[\Gamma]}_1 \int_0^t \|[e^{\widetilde{A}\sigma}]_{1,1}\|\,\mathrm{d}\sigma + \overline{[\Gamma]}_2 \int_0^t \|[e^{\widetilde{A}\sigma}]_{1,2}\|\,\mathrm{d}\sigma, \text{ and} \tag{7.b}$$

$$\|\dot{\lambda}(t)\| \le \overline{[\Gamma]}_1 \int_0^t \|[e^{\widetilde{A}\sigma}]_{2,1}\|\,\mathrm{d}\sigma + \overline{[\Gamma]}_2 \int_0^t \|[e^{\widetilde{A}\sigma}]_{2,2}\|\,\mathrm{d}\sigma. \tag{7.c}$$

The advantage of (7.b) and (7.c) is that they are tighter since they can incorporate $[\Gamma]_1 = 0$, which is the case for all the formation flying models considered.

3.3 - Method 2

This method is used for trajectory validation only as it results in monotonically increasing error bounds. Assume the following structures for A_s, B and Γ:

$$A_s = \left[\begin{array}{c|c} 0 & I \\ \hline H_\lambda & H_{\dot{\lambda}} \end{array}\right], \quad B = \left[\begin{array}{c} 0 \\ \hline I \end{array}\right]$$

and $[\Gamma]_1 = 0$. Letting γ represent $[\Gamma]_2$, we have

$$\|\dot{\lambda}(t)\| \le \int_0^t (\overline{H}_\lambda\bar{\lambda} + \overline{H}_{\dot{\lambda}}\bar{\dot{\lambda}} + \bar{\gamma})\,\mathrm{d}\sigma \quad \text{and} \quad \|\lambda(t)\| \le \int_0^t \int_0^{\sigma_1} (\overline{H}_\lambda\bar{\lambda} + \overline{H}_{\dot{\lambda}}\bar{\dot{\lambda}} + \bar{\gamma})\,\mathrm{d}\sigma_2\,\mathrm{d}\sigma_1.$$

Table 2: Simplified Relative State Error Bounding Process

1) Choose a time interval of interest, $[0, t_f]$ (e.g. for TPF a formation rotation will take 8 hours). 2) Calculate $\bar{x}_{I,s}(t)$ on $[0, t_f]$ (time interval implied hereafter) using (6). 3) Set $t^* = \text{argmax}\{\bar{x}_{I,s}(t)\}$. Based on $\bar{x}_{I,s}(t^*)$, *assume* a value for $\bar{x}_I$. 4) Using the assumed $\bar{x}_I$, calculate $\overline{\Lambda}_I(t)$ using Method 1 (§3.2) or Method 2 (§3.3). 5) Verify $\bar{x}_I \geq \max\{\bar{x}_{I,s}(t) + \overline{\Lambda}_I(t)\}$. Otherwise, assume a larger value for $\bar{x}_I$ and go to Step 4). This process is not guaranteed to lead to a verifiable $\bar{x}_I$.	6) Calculate $\bar{x}_s(t)$ using (6) 7) Set $t^* = \text{argmax}\{\bar{x}_s(t)\}$. Based on $\bar{x}_s(t^*)$, *assume* a value for $\bar{x}$. 8) Using the assumed $\bar{x}$, calculate $\overline{\Lambda}(t)$ using Method 1 or Method 2. 9) Verify $\bar{x} \geq \max\{\bar{x}_s(t) + \overline{\Lambda}(t)\}$. Otherwise, assume a larger value for $\bar{x}$ and go to Step 8). This process is not guaranteed to lead to a verifiable $\bar{x}$. 10) Done. $\overline{\Lambda}(t)$ is a bound on the relative state error for $t \in [0, t_f]$.

Choosing $\bar{\lambda}$ and $\bar{\dot{\lambda}}$ so that these inequalities are just satisfied at time t yields the condition

$$\begin{bmatrix} \overline{H}_{\dot{\lambda}} t - 1 & \overline{H}_{\lambda} t \\ \overline{H}_{\dot{\lambda}} \frac{t^2}{2} & \overline{H}_{\lambda} \frac{t^2}{2} - 1 \end{bmatrix} \begin{bmatrix} \bar{\dot{\lambda}} \\ \bar{\lambda} \end{bmatrix} = \begin{bmatrix} \bar{\gamma} t \\ \bar{\gamma} \frac{t^2}{2} \end{bmatrix}.$$

This equation leads to the following error bounds:

$$\bar{\dot{\lambda}}(t) = \frac{\bar{\gamma} t}{1 - \overline{H}_{\dot{\lambda}} t - \overline{H}_{\lambda} \frac{t^2}{2}} \quad \text{and} \quad \bar{\lambda}(t) = \frac{\bar{\gamma} \frac{t^2}{2}}{1 - \overline{H}_{\dot{\lambda}} t - \overline{H}_{\lambda} \frac{t^2}{2}}.$$

4 - TPF EXAMPLE

These bounds are now calculated for two spacecraft, a Combiner and Collector, in a TPF-based formation. To evaluate the conservatism of the bounds, the truth model is also simulated with 17 digits of integrator accuracy—equivalent to an accuracy of one micrometer at one AU.[4]

We first take $t_f = 1.44e5\ s$ (40 hours). For both trajectory and control validation, spacecraft j, the Combiner, is drifting inertially starting at $x_I^*(0) = 0$ with uncertainties $\overline{[\Delta x_I(0)]}_1 = 10\,m$, $\overline{[\Delta x_I(0)]}_2 = 1\,m/s$ and $\overline{[\Delta \mathcal{D}_{I,s}]}_2$ set to 10% of $\sup_t \|\mathcal{D}_{I,s}^*\|$. $\overline{[\Delta \mathcal{D}_{I,s}]}_1$ is zero. Then from (6), $\bar{x}_{I,s} = 156911.2$. Assuming $\bar{x}_I = 156912$, error bounds are calculated via Method 2. The maximum error is 0.1, and so $\bar{x}_I$ is verified. A truth simulation for an initial condition satisfying the above variational bounds resulted in $\|x_I(t_f)\| = 155303$—$\bar{x}_I$ is only 1% conservative. Spacecraft i, the Collector, is placed $999\,m$ away from O_F in a direction selected heuristically to maximize $\mathcal{D}(t)$. Feedforward control holds it there by canceling the terms in the respective simplified model. Since we are not considering trajectory sensitivity, $\overline{\Delta x(0)} = 0$. We also assume $\overline{\Delta \mathcal{D}}_s = 0$; otherwise a different $\bar{x}_s$ must be calculated for each simplified model. With these assumptions $\bar{x}_s = 999$ is valid for all times—in (6) the first term on the right-hand side equals 999 by construction and the remaining two terms have been assumed to be zero.

Consider trajectory (i.e., open loop control) design in which $K = 0$. Assume $\bar{x} = 1000$. Error bounds are calculated using Method 2. We are only concerned with relative position errors on the order of $1\,cm$. Over the range of time that this is the case, the error bound is less than 1, and so $\bar{x}$ is verified.

In Fig. 4 the error bounds for $\|\lambda\|$ are plotted as dashed lines and the errors as calculated in MATHEMATICA for heuristically selected initial conditions are plotted as dashed lines. Since the error bound does not depend on $u_{ff}(t)$, these bounds tell us the most error incurred by using a simplified model for *any* trajectory design in which the formation has drifted roughly less than

[4]The truth simulations are performed in MATHEMATICA using the NDSolve function. NDSolve uses an Adams Predictor-Corrector with adaptive step size. Internal calculations are set to 27 digits in MATHEMATICA, corresponding to an absolute accuracy goal for NDSolve of 17 digits.

157 km from the reference circular orbit and the error bound plus the simplified relative state bound remains less than 1000. For example, the g_∞-model bound applies to reconfiguration trajectories designed using the closed-form Lambert's solution of the HCW Equations.

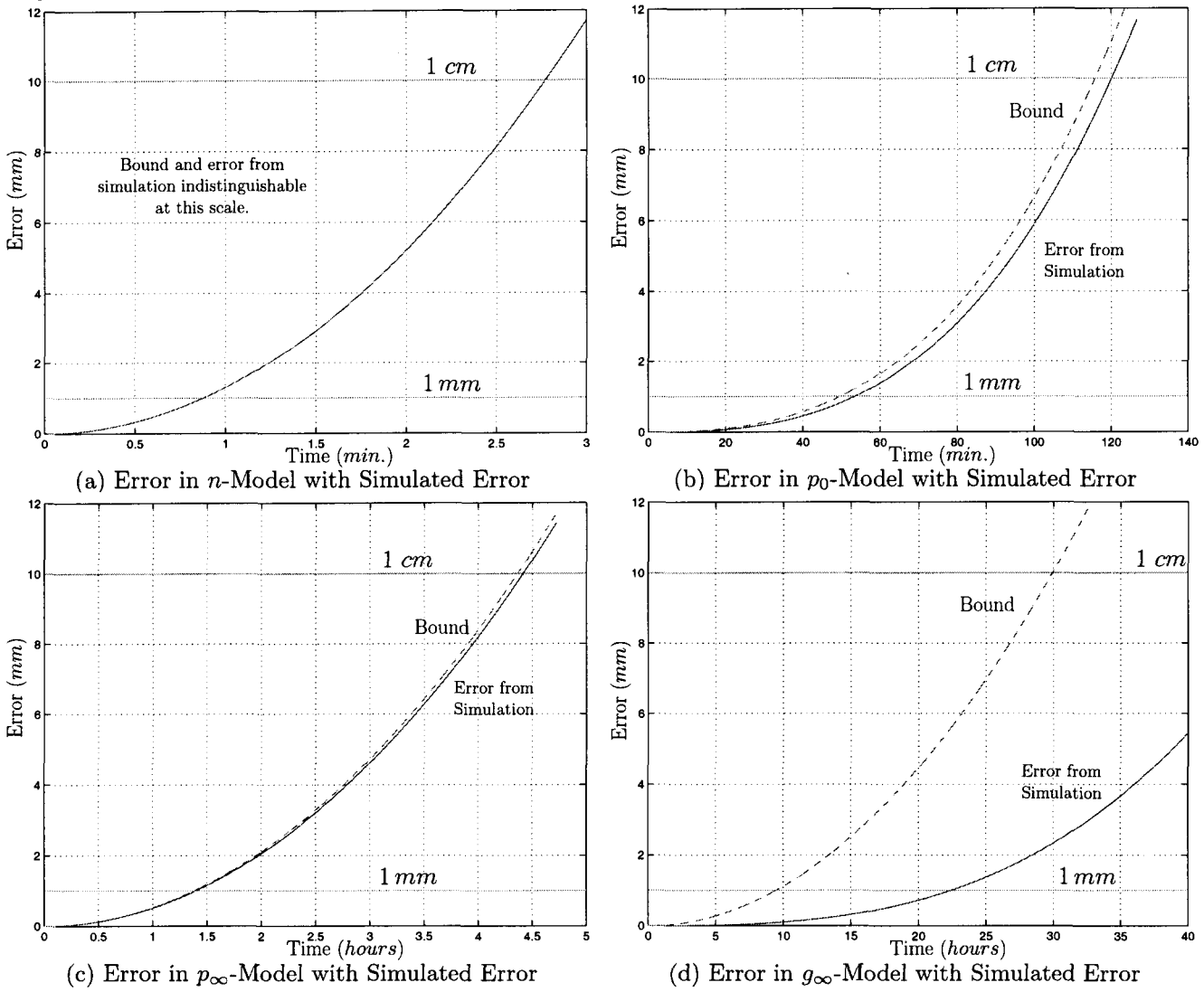

(a) Error in n-Model with Simulated Error

(b) Error in p_0-Model with Simulated Error

(c) Error in p_∞-Model with Simulated Error

(d) Error in g_∞-Model with Simulated Error

Fig. 3: Guidance Error Bound Comparisons for TPF

For feedback controller validation using Method 1, we only consider the n-model for brevity. The Collector is placed 1000 m away from the Combiner and is commanded to the point 1000 m on the other side of the Combiner. C is taken as the identity matrix and two linear-quadratic regulators are designed with identity state weighting matrices. Their control weight matrices are the identity matrix (High-Gain, maximum acceleration in simplified model of $3.2e3\, m/s^2$) and the identity matrix multiplied by $1e14$ (Low-Gain, max. accel. of $2.4e-4\, m/s^2$, consistent with the saturation limit of Table 1), respectively. Shown in Fig. 4 are the error bounds calculated using Method 1 and the actual errors as simulated in MATHEMATICA. From the figure, one sees that if the control authority is large, a simplified model may be used with greater impunity than if the control authority is small—for the low-authority controller design using the disturbance-free free-flying model leads to 8 meters of error.

5 - CONCLUSIONS

The bootstrapping error bounding technique developed in this paper has shown that trajectories designed using a free-flying model with a constant solar pressure disturbance can be accurate to 1 cm for up to 4.5 hours (under some assumptions). This accuracy means that for TPF reconfigurations taking less than 4.5 hours, optimal trajectories can be designed using the free-flying model *without the need to refine them.* Also shown was that trajectories designed using a HCW Equations-based model are accurate to 1 cm for up 30 hours (subject to assumptions).

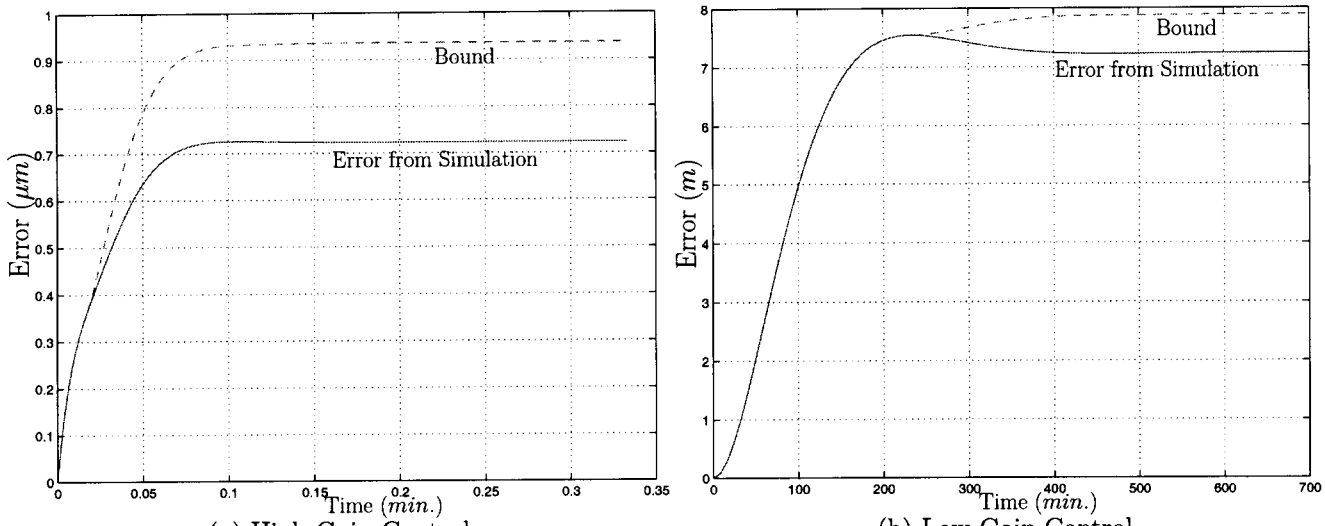

(a) High-Gain Control (b) Low-Gain Control

Fig. 4: n-Model Control Error Bound Comparisons for TPF

The error bounding results for static feedback controllers need to be extended to more realistic control scenarios in which the reference trajectory is fed to the controller in increments—feedback control would not be started with an initial error of $2\,km$. Nonetheless, a method was developed for *quantitatively* bounding the error when a linear output feedback system is applied to a nonlinear truth model. Further, it was shown theoretically that high gain control designs on a free-flying model can have sub-micrometer errors, while low-gain control designs can have errors on the order of meters.

ACKNOWLEDGMENTS. This research was carried out at the Jet Propulsion Laboratory, California Institute of Technology, under a contract with the National Aeronautics and Space Administration. The authors thank Dr. Marco Quadrelli and Dr. Scott Ploen of JPL for helpful discussions.

REFERENCES:

[Bear 01] R.W. Beard, J. Lawton, and F.Y. Hadaegh, "A coordination architecture for spacecraft formation control," *IEEE Trans. Contr. Syst. Tech.*, 9(6):777–790, 2001.

[Beic 99] C.A. Beichman, N.J. Woolf, and C.A. Lindensmith, eds., "The Terrestrial Planet Finder (TPF): A NASA Origins Program to Search for Habitable Planets," JPL Pub. 99-3, Cal. Inst. of Tech., Pasadena, CA, 1999.

[deQu 00] M.S. de Queiroz, V. Kapila, and Q. Yan, "Adaptive nonlinear control of multiple spacecraft formation flying," *J. Guid., Contr., & Dyn.*, 23(3):385–390, 2000.

[DeCo 91] A.B. DeCou, "Orbital station-keeping for multiple spacecraft interferometry," *J. Astronaut. Sci.*, 39(3):283–297, 1991.

[Hada 00] F.Y. Hadaegh, A.R. Ghavimi, G. Singh, and M. Quadrelli, "A centralized optimal controller for formation flying spacecraft," in *Intrntl. Conf. Intel. Tech.*, 2000.

[Hada 01] F.Y. Hadaegh, D.P. Scharf, and B. Kang, "Rule-based estimation and control for formation flying," in *Intrntl. Conf. on Intel. Technologies*, Bangkok, Thailand, 2001.

[Mesb 01] M. Mesbahi and F.Y. Hadaegh, "Mode and logic-based switching for the control of separated spacecraft optical interferometers," *J. Astro. Sci.*, 49(3,4), 2001.

[Rao 01] V.G. Rao and D.S. Bernstein, "Naive control of the double integrator," *IEEE Contr. Syst. Magazine*, 21(5):86–97, 2001.

[Vall 97] D.A. Vallado and W.D. McClain, *Fundamentals of Astrodynamics and Applications.* McGraw-Hill, New York, NY, 1997.

[Vass 85] R.H. Vassar and R.B. Sherwood, "Formationkeeping for a pair of satellites in a circular orbit," *J. Guid., Contr., & Dyn.*, 8(2):235–242, 1985.

[Wang 99] P.K.C. Wang and F.Y. Hadaegh, "Minimum-fuel formation reconfiguration of multiple free-flying spacecraft," *J. Astronaut. Sci.*, 47(1,2):77–102, 1999.